

Search for $\psi(3686) \rightarrow \gamma\eta_c(\eta(1405)) \rightarrow \gamma\pi^+\pi^-\pi^0$

M. Ablikim,¹ M. N. Achasov,^{9,e} S. Ahmed,¹⁴ M. Albrecht,⁴ A. Amoroso,^{50a,50c} F. F. An,¹ Q. An,^{47,39} J. Z. Bai,¹ O. Bakina,²⁴ R. Baldini Ferroli,^{20a} Y. Ban,³² D. W. Bennett,¹⁹ J. V. Bennett,⁵ N. Berger,²³ M. Bertani,^{20a} D. Bettoni,^{21a} J. M. Bian,⁴⁵ F. Bianchi,^{50a,50c} E. Boger,^{24,c} I. Boyko,²⁴ R. A. Briere,⁵ H. Cai,⁵² X. Cai,^{1,39} O. Cakir,^{42a} A. Calcaterra,^{20a} G. F. Cao,^{1,43} S. A. Cetin,^{42b} J. Chai,^{50c} J. F. Chang,^{1,39} G. Chelkov,^{24,c,d} G. Chen,¹ H. S. Chen,^{1,43} J. C. Chen,¹ M. L. Chen,^{1,39} S. J. Chen,³⁰ X. R. Chen,²⁷ Y. B. Chen,^{1,39} X. K. Chu,³² G. Cibinetto,^{21a} H. L. Dai,^{1,39} J. P. Dai,^{35,i} A. Dbeyssi,¹⁴ D. Dedovich,²⁴ Z. Y. Deng,¹ A. Denig,²³ I. Denysenko,²⁴ M. Destefanis,^{50a,50c} F. De Mori,^{50a,50c} Y. Ding,²⁸ C. Dong,³¹ J. Dong,^{1,39} L. Y. Dong,^{1,43} M. Y. Dong,^{1,39,43} O. Dorjkhaidav,²² Z. L. Dou,³⁰ S. X. Du,⁵⁴ P. F. Duan,¹ J. Fang,^{1,39} S. S. Fang,^{1,43} X. Fang,^{47,39} Y. Fang,¹ R. Farinelli,^{21a,21b} L. Fava,^{50b,50c} S. Fegan,²³ F. Feldbauer,²³ G. Felici,^{20a} C. Q. Feng,^{47,39} E. Fioravanti,^{21a} M. Fritsch,^{23,14} C. D. Fu,¹ Q. Gao,¹ X. L. Gao,^{47,39} Y. Gao,⁴¹ Y. G. Gao,⁶ Z. Gao,^{47,39} I. Garzia,^{21a} K. Goetzen,¹⁰ L. Gong,³¹ W. X. Gong,^{1,39} W. Gradl,²³ M. Greco,^{50a,50c} M. H. Gu,^{1,39} S. Gu,^{15,a} Y. T. Gu,¹² A. Q. Guo,¹ L. B. Guo,²⁹ R. P. Guo,¹ Y. P. Guo,²³ Z. Haddadi,²⁶ A. Hafner,²³ S. Han,⁵² X. Q. Hao,¹⁵ F. A. Harris,⁴⁴ K. L. He,^{1,43} X. Q. He,⁴⁶ F. H. Heinsius,⁴ T. Held,⁴ Y. K. Heng,^{1,39,43} T. Holtmann,⁴ Z. L. Hou,¹ C. Hu,²⁹ H. M. Hu,^{1,43} T. Hu,^{1,39,43} Y. Hu,¹ G. S. Huang,^{47,39} J. S. Huang,¹⁵ X. T. Huang,³⁴ X. Z. Huang,³⁰ Z. L. Huang,²⁸ T. Hussain,⁴⁹ W. Ikegami Andersson,⁵¹ Q. Ji,¹ Q. P. Ji,¹⁵ X. B. Ji,^{1,43} X. L. Ji,^{1,39} X. S. Jiang,^{1,39,43} X. Y. Jiang,³¹ J. B. Jiao,³⁴ Z. Jiao,¹⁷ D. P. Jin,^{1,39,43} S. Jin,^{1,43} T. Johansson,⁵¹ A. Julin,⁴⁵ N. Kalantar-Nayestanaki,²⁶ X. L. Kang,¹ X. S. Kang,³¹ M. Kavatsyuk,²⁶ B. C. Ke,⁵ T. Khan,^{47,39} P. Kiese,²³ R. Kliemt,¹⁰ B. Kloss,²³ L. Koch,²⁵ O. B. Kolcu,^{42b,g} B. Kopf,⁴ M. Kornicer,⁴⁴ M. Kuemmel,⁴ M. Kuhlmann,⁴ A. Kupsc,⁵¹ W. Kühn,²⁵ J. S. Lange,²⁵ M. Lara,¹⁹ P. Larin,¹⁴ L. Lavezzi,^{50c} H. Leithoff,²³ C. Leng,^{50c} C. Li,⁵¹ Cheng Li,^{47,39} D. M. Li,⁵⁴ F. Li,^{1,39} F. Y. Li,³² G. Li,¹ H. B. Li,^{1,43} H. J. Li,¹ J. C. Li,¹ Jin Li,³³ Kang Li,¹³ Ke Li,³⁴ Lei Li,³ P. L. Li,^{47,39} P. R. Li,^{43,7} Q. Y. Li,³⁴ T. Li,³⁴ W. D. Li,^{1,43} W. G. Li,¹ X. L. Li,³⁴ X. N. Li,^{1,39} X. Q. Li,³¹ Z. B. Li,⁴⁰ H. Liang,^{47,39} Y. F. Liang,³⁷ Y. T. Liang,²⁵ G. R. Liao,¹¹ D. X. Lin,¹⁴ B. Liu,^{35,i} B. J. Liu,¹ C. X. Liu,¹ D. Liu,^{47,39} F. H. Liu,³⁶ Fang Liu,¹ Feng Liu,⁶ H. B. Liu,¹² H. M. Liu,^{1,43} Huanhuan Liu,¹ Huihui Liu,¹⁶ J. B. Liu,^{47,39} J. P. Liu,⁵² J. Y. Liu,¹ K. Liu,⁴¹ K. Y. Liu,²⁸ Ke Liu,⁶ L. D. Liu,³² P. L. Liu,^{1,39} Q. Liu,⁴³ S. B. Liu,^{47,39} X. Liu,²⁷ Y. B. Liu,³¹ Y. Y. Liu,³¹ Z. A. Liu,^{1,39,43} Zhiqing Liu,²³ Y. F. Long,³² X. C. Lou,^{1,39,43} H. J. Lu,¹⁷ J. G. Lu,^{1,39} Y. Lu,¹ Y. P. Lu,^{1,39} C. L. Luo,²⁹ M. X. Luo,⁵³ T. Luo,⁴⁴ X. L. Luo,^{1,39} X. R. Lyu,⁴³ F. C. Ma,²⁸ H. L. Ma,¹ L. L. Ma,³⁴ M. M. Ma,¹ Q. M. Ma,¹ T. Ma,¹ X. N. Ma,³¹ X. Y. Ma,^{1,39} Y. M. Ma,³⁴ F. E. Maas,¹⁴ M. Maggiora,^{50a,50c} Q. A. Malik,⁴⁹ Y. J. Mao,³² Z. P. Mao,¹ S. Marcelllo,^{50a,50c} J. G. Messchendorp,²⁶ G. Mezzadri,^{21b} J. Min,^{1,39} T. J. Min,¹ R. E. Mitchell,¹⁹ X. H. Mo,^{1,39,43} Y. J. Mo,⁶ C. Morales Morales,¹⁴ G. Morello,^{20a} N. Yu. Muchnoi,^{9,e} H. Muramatsu,⁴⁵ P. Musiol,⁴ A. Mustafa,⁴ Y. Nefedov,²⁴ F. Nerling,¹⁰ I. B. Nikolaev,^{9,e} Z. Ning,^{1,39} S. Nisar,⁸ S. L. Niu,^{1,39} X. Y. Niu,¹ S. L. Olsen,³³ Q. Ouyang,^{1,39,43} S. Pacetti,^{20b} Y. Pan,^{47,39} M. Papenbrock,⁵¹ P. Patteri,^{20a} M. Pelizaeus,⁴ J. Pellegrino,^{50a,50c} H. P. Peng,^{47,39} K. Peters,^{10,h} J. Pettersson,⁵¹ J. L. Ping,²⁹ R. G. Ping,^{1,43} R. Poling,⁴⁵ V. Prasad,^{47,39} H. R. Qi,² M. Qi,³⁰ S. Qian,^{1,39} C. F. Qiao,⁴³ J. J. Qin,⁴³ N. Qin,⁵² X. S. Qin,¹ Z. H. Qin,^{1,39} J. F. Qiu,¹ K. H. Rashid,^{49,j} C. F. Redmer,²³ M. Richter,⁴ M. Ripka,²³ G. Rong,^{1,43} Ch. Rosner,¹⁴ X. D. Ruan,¹² A. Sarantsev,^{24,f} M. Savrié,^{21b} C. Schnier,⁴ K. Schoenning,⁵¹ W. Shan,³² M. Shao,^{47,39} C. P. Shen,² P. X. Shen,³¹ X. Y. Shen,^{1,43} H. Y. Sheng,¹ J. J. Song,³⁴ W. M. Song,³⁴ X. Y. Song,¹ S. Sosio,^{50a,50c} C. Sowa,⁴ S. Spataro,^{50a,50c} G. X. Sun,¹ J. F. Sun,¹⁵ S. S. Sun,^{1,43} X. H. Sun,¹ Y. J. Sun,^{47,39} Y. K. Sun,^{47,39} Y. Z. Sun,¹ Z. J. Sun,^{1,39} Z. T. Sun,¹⁹ C. J. Tang,³⁷ G. Y. Tang,¹ X. Tang,¹ I. Tapan,^{42c} M. Tiemens,²⁶ B. T. Tsednee,²² I. Uman,^{42d} G. S. Varner,⁴⁴ B. Wang,¹ B. L. Wang,⁴³ D. Wang,³² D. Y. Wang,³² Dan Wang,⁴³ K. Wang,^{1,39} L. L. Wang,¹ L. S. Wang,¹ M. Wang,³⁴ P. Wang,¹ P. L. Wang,¹ W. P. Wang,^{47,39} X. F. Wang,⁴¹ Y. Wang,³⁸ Y. D. Wang,¹⁴ Y. F. Wang,^{1,39,43} Y. Q. Wang,²⁵ Z. Wang,^{1,39} Z. G. Wang,^{1,39} Z. H. Wang,^{47,39} Z. Y. Wang,¹ Zongyuan Wang,¹ T. Weber,²³ D. H. Wei,¹¹ J. H. Wei,³¹ P. Weidenkaff,²³ S. P. Wen,¹ U. Wiedner,⁴ M. Wolke,⁵¹ L. H. Wu,¹ L. J. Wu,¹ Z. Wu,^{1,39} L. Xia,^{47,39} Y. Xia,¹⁸ D. Xiao,¹ H. Xiao,⁴⁸ Y. J. Xiao,¹ Z. J. Xiao,²⁹ Y. G. Xie,^{1,39} Y. H. Xie,⁶ X. A. Xiong,¹ Q. L. Xiu,^{1,39} G. F. Xu,¹ J. J. Xu,¹ L. Xu,¹ Q. J. Xu,¹³ Q. N. Xu,⁴³ X. P. Xu,³⁸ L. Yan,^{50a,50c} W. B. Yan,^{47,39} W. C. Yan,^{47,39} Y. H. Yan,¹⁸ H. J. Yang,^{35,i} H. X. Yang,¹ L. Yang,⁵² Y. H. Yang,³⁰ Y. X. Yang,¹¹ M. Ye,^{1,39} M. H. Ye,⁷ J. H. Yin,¹ Z. Y. You,⁴⁰ B. X. Yu,^{1,39,43} C. X. Yu,³¹ J. S. Yu,²⁷ C. Z. Yuan,^{1,43} Y. Yuan,¹ A. Yuncu,^{42b,b} A. A. Zafar,⁴⁹ Y. Zeng,¹⁸ Z. Zeng,^{47,39} B. X. Zhang,¹ B. Y. Zhang,^{1,39} C. C. Zhang,¹ D. H. Zhang,¹ H. H. Zhang,⁴⁰ H. Y. Zhang,^{1,39} J. Zhang,¹ J. L. Zhang,¹ J. Q. Zhang,¹ J. W. Zhang,^{1,39,43} J. Y. Zhang,¹ J. Z. Zhang,^{1,43} K. Zhang,¹ L. Zhang,⁴¹ S. Q. Zhang,³¹ X. Y. Zhang,³⁴ Y. H. Zhang,^{1,39} Y. T. Zhang,^{47,39} Yang Zhang,¹ Yao Zhang,¹ Yu Zhang,⁴³ Z. H. Zhang,⁶ Z. P. Zhang,⁴⁷ Z. Y. Zhang,⁵² G. Zhao,¹ J. W. Zhao,^{1,39} J. Y. Zhao,¹ J. Z. Zhao,^{1,39} Lei Zhao,^{47,39} Ling Zhao,¹ M. G. Zhao,³¹ Q. Zhao,¹ S. J. Zhao,⁵⁴ T. C. Zhao,¹ Y. B. Zhao,^{1,39} Z. G. Zhao,^{47,39} A. Zhemchugov,^{24,c} B. Zheng,^{48,14} J. P. Zheng,^{1,39} W. J. Zheng,³⁴ Y. H. Zheng,⁴³ B. Zhong,²⁹ L. Zhou,^{1,39} X. Zhou,⁵² X. K. Zhou,^{47,39} X. R. Zhou,^{47,39} X. Y. Zhou,¹ Y. X. Zhou,¹² K. Zhu,¹ K. J. Zhu,^{1,39,43} S. Zhu,¹ S. H. Zhu,⁴⁶ X. L. Zhu,⁴¹ Y. C. Zhu,^{47,39} Y. S. Zhu,^{1,43} Z. A. Zhu,^{1,43} J. Zhuang,^{1,39} L. Zotti,^{50a,50c} B. S. Zou,¹ and J. H. Zou¹

(BESIII Collaboration)

- ¹*Institute of High Energy Physics, Beijing 100049, People's Republic of China*
²*Beihang University, Beijing 100191, People's Republic of China*
³*Beijing Institute of Petrochemical Technology, Beijing 102617, People's Republic of China*
⁴*Bochum Ruhr-University, D-44780 Bochum, Germany*
⁵*Carnegie Mellon University, Pittsburgh, Pennsylvania 15213, USA*
⁶*Central China Normal University, Wuhan 430079, People's Republic of China*
⁷*China Center of Advanced Science and Technology, Beijing 100190, People's Republic of China*
⁸*COMSATS Institute of Information Technology, Lahore, Defence Road, Off Raiwind Road, 54000 Lahore, Pakistan*
⁹*G.I. Budker Institute of Nuclear Physics SB RAS (BINP), Novosibirsk 630090, Russia*
¹⁰*GSI Helmholtzcentre for Heavy Ion Research GmbH, D-64291 Darmstadt, Germany*
¹¹*Guangxi Normal University, Guilin 541004, People's Republic of China*
¹²*Guangxi University, Nanning 530004, People's Republic of China*
¹³*Hangzhou Normal University, Hangzhou 310036, People's Republic of China*
¹⁴*Helmholtz Institute Mainz, Johann-Joachim-Becher-Weg 45, D-55099 Mainz, Germany*
¹⁵*Henan Normal University, Xinxiang 453007, People's Republic of China*
¹⁶*Henan University of Science and Technology, Luoyang 471003, People's Republic of China*
¹⁷*Huangshan College, Huangshan 245000, People's Republic of China*
¹⁸*Hunan University, Changsha 410082, People's Republic of China*
¹⁹*Indiana University, Bloomington, Indiana 47405, USA*
^{20a}*INFN Laboratori Nazionali di Frascati, I-00044 Frascati, Italy*
^{20b}*INFN and University of Perugia, I-06100 Perugia, Italy*
^{21a}*INFN Sezione di Ferrara, I-44122 Ferrara, Italy*
^{21b}*University of Ferrara, I-44122 Ferrara, Italy*
²²*Institute of Physics and Technology, Peace Ave. 54B, Ulaanbaatar 13330, Mongolia*
²³*Johannes Gutenberg University of Mainz, Johann-Joachim-Becher-Weg 45, D-55099 Mainz, Germany*
²⁴*Joint Institute for Nuclear Research, 141980 Dubna, Moscow region, Russia*
²⁵*Justus-Liebig-Universitaet Giessen, II. Physikalisches Institut, Heinrich-Buff-Ring 16, D-35392 Giessen, Germany*
²⁶*KVI-CART, University of Groningen, NL-9747 AA Groningen, Netherlands*
²⁷*Lanzhou University, Lanzhou 730000, People's Republic of China*
²⁸*Liaoning University, Shenyang 110036, People's Republic of China*
²⁹*Nanjing Normal University, Nanjing 210023, People's Republic of China*
³⁰*Nanjing University, Nanjing 210093, People's Republic of China*
³¹*Nankai University, Tianjin 300071, People's Republic of China*
³²*Peking University, Beijing 100871, People's Republic of China*
³³*Seoul National University, Seoul 151-747, Korea*
³⁴*Shandong University, Jinan 250100, People's Republic of China*
³⁵*Shanghai Jiao Tong University, Shanghai 200240, People's Republic of China*
³⁶*Shanxi University, Taiyuan 030006, People's Republic of China*
³⁷*Sichuan University, Chengdu 610064, People's Republic of China*
³⁸*Soochow University, Suzhou 215006, People's Republic of China*
³⁹*State Key Laboratory of Particle Detection and Electronics, Beijing 100049, Hefei 230026, People's Republic of China*
⁴⁰*Sun Yat-Sen University, Guangzhou 510275, People's Republic of China*
⁴¹*Tsinghua University, Beijing 100084, People's Republic of China*
^{42a}*Ankara University, 06100 Tandogan, Ankara, Turkey*
^{42b}*Istanbul Bilgi University, 34060 Eyup, Istanbul, Turkey*
^{42c}*Uludag University, 16059 Bursa, Turkey*
^{42d}*Near East University, Nicosia, North Cyprus, Mersin 10, Turkey*
⁴³*University of Chinese Academy of Sciences, Beijing 100049, People's Republic of China*
⁴⁴*University of Hawaii, Honolulu, Hawaii 96822, USA*
⁴⁵*University of Minnesota, Minneapolis, Minnesota 55455, USA*
⁴⁶*University of Science and Technology Liaoning, Anshan 114051, People's Republic of China*
⁴⁷*University of Science and Technology of China, Hefei 230026, People's Republic of China*
⁴⁸*University of South China, Hengyang 421001, People's Republic of China*
⁴⁹*University of the Punjab, Lahore-54590, Pakistan*
^{50a}*University of Turin, I-10125 Turin, Italy*
^{50b}*University of Eastern Piedmont, I-15121 Alessandria, Italy*
^{50c}*INFN, I-10125 Turin, Italy*

⁵¹*Uppsala University, Box 516, SE-75120 Uppsala, Sweden*⁵²*Wuhan University, Wuhan 430072, People's Republic of China*⁵³*Zhejiang University, Hangzhou 310027, People's Republic of China*⁵⁴*Zhengzhou University, Zhengzhou 450001, People's Republic of China*
(Received 18 July 2017; published 20 December 2017)

Using a sample of 448.1×10^6 $\psi(3686)$ events collected with the BESIII detector, a search for the isospin violating decay $\eta_c \rightarrow \pi^+ \pi^- \pi^0$ via $\psi(3686) \rightarrow \gamma \eta_c$ is presented. No signal is observed, and the upper limit on $\mathcal{B}(\psi(3686) \rightarrow \gamma \eta_c) \times \mathcal{B}(\eta_c \rightarrow \pi^+ \pi^- \pi^0)$ is determined to be 1.6×10^{-6} at the 90% confidence level. In addition, a search for $\eta(1405) \rightarrow f_0(980) \pi^0$ in $\psi(3686)$ radiative decays is performed. No signal is observed, and the branching fraction $\mathcal{B}(\psi(3686) \rightarrow \gamma \eta(1405)) \times \mathcal{B}(\eta(1405) \rightarrow f_0(980) \pi^0) \times \mathcal{B}(f_0(980) \rightarrow \pi^+ \pi^-)$ is calculated to be less than 5.0×10^{-7} at the 90% confidence level.

DOI: 10.1103/PhysRevD.96.112008

I. INTRODUCTION

As the lowest-lying $c\bar{c}$ state, the pseudoscalar meson η_c has attracted considerable theoretical and experimental attention since it was discovered three decades ago [1]. To the lowest order in perturbation theory, the η_c decays through $c\bar{c}$ annihilation into two gluons. The η_c is then expected to have numerous hadronic decay modes into two- or three-body hadronic final states, and many of them have been measured [2]. However, the three-pion decay mode has not yet been studied, but its measurement is important to test isospin symmetry [3–5].

Charmonium radiative decays, especially those of J/ψ and $\psi(3686)$, provide an excellent laboratory for the study of neutral pseudoscalar meson decays. For example, the BESIII experiment using J/ψ radiative decays has performed a series of analyses on three pion decays [6–11], and for the first time reported the observation of the isospin violating decay $\eta(1405) \rightarrow 3\pi$ [12]. Of particular interest in $\eta(1405) \rightarrow 3\pi$ decay is a narrow structure around $0.98 \text{ GeV}/c^2$ in the $\pi\pi$ mass spectrum, identified with

the $f_0(980)$, which can be interpreted under the triangle singularity scheme [13–15].

In this analysis, we perform a search for the isospin violating decay $\eta_c \rightarrow \pi^+ \pi^- \pi^0$ using a sample of 448.1×10^6 $\psi(3686)$ events [16] collected with the BESIII [17] detector operating at the BEPCII [18] storage ring. We also perform a search for $\eta(1405) \rightarrow f_0(980) \pi^0$ in the $\psi(3686)$ radiative decays to test the “12% rule” [19–21], in which perturbative QCD predicts the ratio of the branching fractions of $\psi(3686)$ and J/ψ into the same final hadronic state is given

$$Q = \frac{\mathcal{B}_{\psi(3686) \rightarrow h}}{\mathcal{B}_{J/\psi \rightarrow h}} = \frac{\mathcal{B}_{\psi(3686) \rightarrow l^+ l^-}}{\mathcal{B}_{J/\psi \rightarrow l^+ l^-}} \approx (12.4 \pm 0.4)\%. \quad (1)$$

The rule is expected to also hold for radiative decays to the same final hadronic state.

II. DETECTOR AND MONTE CARLO SIMULATION

BEPCII is a double-ring e^+e^- collider providing a peak luminosity of $10^{33} \text{ cm}^{-2} \text{ s}^{-1}$ at a beam energy of 1.89 GeV. The BESIII detector [17] consists of a helium-based main drift chamber (MDC), a plastic scintillator time-of-flight (TOF) system, a CsI(Tl) electromagnetic calorimeter (EMC), and a multilayer resistive plate chamber muon counter system. With a geometrical acceptance of 93% of 4π , the BESIII detector operates in a magnetic field of 1.0 T provided by a superconducting solenoidal magnet.

Monte Carlo (MC) simulations are used to determine detector efficiency, optimize event selection and estimate backgrounds. The BESIII detector is modeled with GEANT4 [22]. For the inclusive MC, the production of the $\psi(3686)$ resonance is simulated by the MC event generator KKMC [23,24], and the decays are generated by EVTGEN [25,26] for known decay modes with branching fractions being set to Particle Data Group (PDG) [2] world average values, while the remaining unknown decays are generated by LUNDCHARM [27]. For $\psi(3686) \rightarrow \gamma \eta_c$, $\eta_c \rightarrow \pi^+ \pi^- \pi^0$ decays, the line shape of the η_c meson is described by $E_\gamma^2 \times |BW(m)|^2 \times D(E_\gamma)$, where m is the $\pi^+ \pi^- \pi^0$ invariant

^aCorresponding author.
gushan@ihep.ac.cn.

^bAlso at Bogazici University, 34342 Istanbul, Turkey.

^cAlso at the Moscow Institute of Physics and Technology, Moscow 141700, Russia.

^dAlso at the Functional Electronics Laboratory, Tomsk State University, Tomsk 634050, Russia.

^eAlso at the Novosibirsk State University, Novosibirsk 630090, Russia.

^fAlso at the NRC “Kurchatov Institute”, PNPI, 188300 Gatchina, Russia.

^gAlso at Istanbul Arel University, 34295 Istanbul, Turkey.

^hAlso at Goethe University Frankfurt, 60323 Frankfurt am Main, Germany.

ⁱAlso at Key Laboratory for Particle Physics, Astrophysics and Cosmology, Ministry of Education; Shanghai Key Laboratory for Particle Physics and Cosmology; Institute of Nuclear and Particle Physics, Shanghai 200240, People's Republic of China.

^jGovernment College Women University, Sialkot - 51310. Punjab, Pakistan.

mass, $E_\gamma = \frac{M_{\psi(3686)}^2 - m^2}{2M_{\psi(3686)}}$ is the energy of the transition photon in the rest frame of $\psi(3686)$, $BW(m) = \frac{1}{m^2 - M_{\eta_c}^2 + iM_{\eta_c}\Gamma_{\eta_c}}$ is a relativistic Breit-Wigner function, M_{η_c} and Γ_{η_c} are the mass and width of η_c , $D(E_\gamma) = \frac{E_0^2}{E_0 E_\gamma + (E_0 - E_\gamma)^2}$ is a function introduced by the KEDR Collaboration [28], which damps the low-mass divergent tail, where $E_0 = \frac{M_{\psi(3686)}^2 - M_{\eta_c}^2}{2M_{\psi(3686)}}$ is the peak energy of the transition photon. In the MC simulation, $\eta_c \rightarrow \pi^+\pi^-\pi^0$ events are generated according to a phase space distribution.

III. DATA ANALYSIS

A. $\psi(3686) \rightarrow \gamma\eta_c, \eta_c \rightarrow \pi^+\pi^-\pi^0$

For $\psi(3686) \rightarrow \gamma\eta_c$ with η_c subsequently decaying into $\pi^+\pi^-\pi^0$, the final state in this analysis is $\pi^+\pi^-\gamma\gamma\gamma$. Charged tracks must be in the active region of the MDC, corresponding to $|\cos\theta| < 0.93$, where θ is the polar angle of the charged track with respect to the beam direction, and are required to pass within ± 10 cm of the interaction point in the beam direction and 1 cm of the beam line in the plane perpendicular to the beam. Photon candidates must have minimum energies of 25 MeV in the EMC barrel ($|\cos\theta| < 0.8$) or 50 MeV in the EMC end caps ($0.86 < |\cos\theta| < 0.92$). To eliminate photons radiated from charged particles, each photon must be separated by at least 10° from any charged track. A requirement on the photon time, TDC , in the EMC, $0 \leq TDC \leq 14$ (50 ns/count), is used to suppress noise and energy deposits unrelated to the event. Events with two oppositely charged tracks and at least three photons are selected for further analysis. The two charged tracks are required to be identified as pions using the combined information of dE/dx from the MDC and the flight time from the TOF.

A four-constraint (4C) kinematic fit imposing energy-momentum conservation is performed under the $\gamma\gamma\pi^+\pi^-$ hypothesis, and the fit results are used for the kinematic quantities below. If there are more than three photon candidates in an event, the combination with the smallest χ_{4C}^2 is retained, and χ_{4C}^2 is required to be less than 20. To suppress the background events with two or four photons in the final states, 4C kinematic fits are also performed under the $\gamma\gamma\pi^+\pi^-$ and $\gamma\gamma\gamma\pi^+\pi^-$ hypotheses, and χ_{4C}^2 is required to be less than the χ^2 values of the $\gamma\gamma\pi^+\pi^-$ and $\gamma\gamma\gamma\pi^+\pi^-$ hypotheses. To select π^0 candidates, the invariant mass of two photons, $M_{\gamma\gamma}$, must satisfy $|M_{\gamma\gamma} - m_{\pi^0}| < 0.015 \text{ GeV}/c^2$, where m_{π^0} is the nominal π^0 mass [2]. If more than one $\gamma\gamma$ combination satisfies this requirement, the one with $M_{\gamma\gamma}$ closest to m_{π^0} is selected. To reject background events with an η in the final state, we require that the invariant masses of the other two possible photon pairs are not within the η mass region, $|M_{\gamma\gamma} - m_\eta| > 0.02 \text{ GeV}/c^2$, where m_η is the

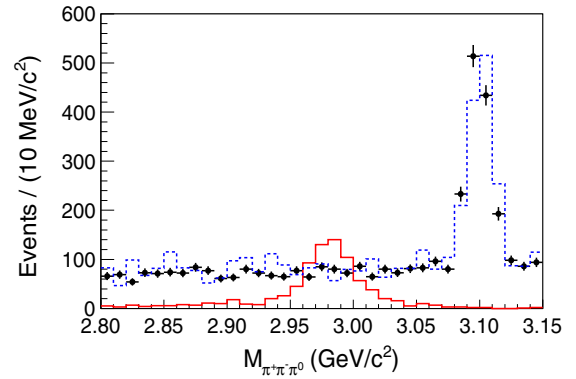


FIG. 1. The distributions of $M_{\pi^+\pi^-\pi^0}$ in the vicinity of the η_c . Dots with error bars are data, the solid line histogram is the η_c line shape from the exclusive MC simulation, and the dashed line are the backgrounds estimated from inclusive MC sample and initial state radiation process $e^+e^- \rightarrow \gamma_{\text{ISR}}J/\psi$.

nominal η mass [2]. In order to reduce the $\omega \rightarrow \gamma\pi^0$ background, $|M_{\gamma\pi^0} - m_\omega| > 0.05 \text{ GeV}/c^2$ is required, where $M_{\gamma\pi^0}$ and m_ω are the $\gamma\pi^0$ invariant mass and nominal ω mass [2], respectively. Events with a $\gamma\pi^+\pi^-$ invariant mass in the vicinity of the J/ψ ($|M_{\gamma\pi^+\pi^-} - m_{J/\psi}| < 0.02 \text{ GeV}/c^2$) are vetoed to suppress background events from $\psi(3686) \rightarrow \pi^0 J/\psi$ ($J/\psi \rightarrow \gamma\pi^+\pi^-$ or $J/\psi \rightarrow \pi^+\pi^-\pi^0$ with a missing photon from the π^0).

After the above requirements, the $M_{\pi^+\pi^-\pi^0}$ distribution is shown in Fig. 1, where no clear η_c signal is seen. Possible backgrounds are studied with an inclusive MC sample of 5.06×10^8 $\psi(3686)$ decays, and the background events contributing to the J/ψ peak in Fig. 1 are dominantly from $\psi(3686) \rightarrow \pi^0 J/\psi$, $J/\psi \rightarrow \pi^+\pi^-\pi^0$ and $\psi(3686) \rightarrow \gamma\chi_{cJ}$, $\chi_{cJ} \rightarrow \gamma J/\psi$, $J/\psi \rightarrow \pi^+\pi^-\pi^0$, while the other background events, mainly from $\psi(3686) \rightarrow \rho\pi\pi$, contribute a smooth shape in the η_c mass region. Using the off resonance continuum data sample taken at a center-of-mass energy of 3.65 GeV, corresponding an integrated luminosity of 44 pb^{-1} [29], we also investigate the background events from QED processes. There are no peaking contributions except for a small J/ψ peak due to the initial state radiation process $e^+e^- \rightarrow \gamma_{\text{ISR}}J/\psi$.

We perform an unbinned maximum likelihood fit to the $M_{\pi^+\pi^-\pi^0}$ distribution in the range of $[2.80, 3.15] \text{ GeV}/c^2$. In the fit, the η_c signal shape is obtained from exclusive MC samples, the J/ψ background shape is described by a Breit-Wigner function convolved with a Gaussian function, and the smooth background is described by a second order Chebychev polynomial function, where all the parameters are free. The fit, shown in Fig. 2, yields $N = 15 \pm 44$ η_c -candidate events, consistent with zero. To obtain an upper limit on the signal yield, a series of unbinned maximum likelihood fits to the $M_{\pi^+\pi^-\pi^0}$ distribution are performed for different values N of the η_c signal yield. The upper limit on N at the 90% confidence level (C.L.), $N_{\eta_c}^{UL}$, is the value of

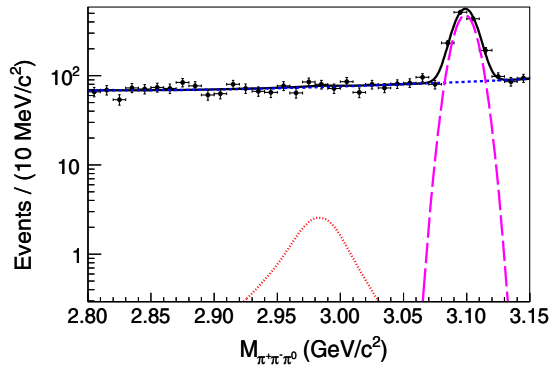


FIG. 2. The result of the fit on the $\pi^+\pi^-\pi^0$ mass spectrum in the η_c region. Dots with error bars are data, the solid curve shows the result of unbinned maximum likelihood fit, the dotted curve is the η_c signal, the long-dashed curve is the J/ψ background, and the short-dashed curve is the main background.

N yielding 90% of the integral of the likelihood over all non-negative values of N . The fit-related uncertainties on $N_{\eta_c}^{UL}$ are considered by varying fit ranges, changing the order of the Chebychev polynomial function for the background shape and changing the mass and width of the η_c within one standard deviation from the central values for the signal shape. The maximum upper limit amongst the variations, $N_{\eta_c}^{UL} = 121$, is used to calculate the upper limit on the branching fraction.

B. $\psi(3686) \rightarrow \gamma\eta(1405)$, $\eta(1405) \rightarrow f_0(980)\pi^0$

The final state for $\psi(3686) \rightarrow \gamma\eta(1405)$, $\eta(1405) \rightarrow f_0(980)\pi^0$ with $f_0(980) \rightarrow \pi^+\pi^-$ is also $\pi^+\pi^-\pi^0$, so we also perform a search for $\eta(1405) \rightarrow f_0(980)\pi^0$ in $\psi(3686)$ radiative decays. The same event selection is used for events with $\pi^+\pi^-\pi^0$ invariant mass within the region of $[1.20, 2.00]$ GeV/c^2 , and the resulting $\pi^+\pi^-$ invariant mass distribution is shown in Fig. 3. A narrow structure around $0.98 \text{ GeV}/c^2$ is observed, which is consistent with that

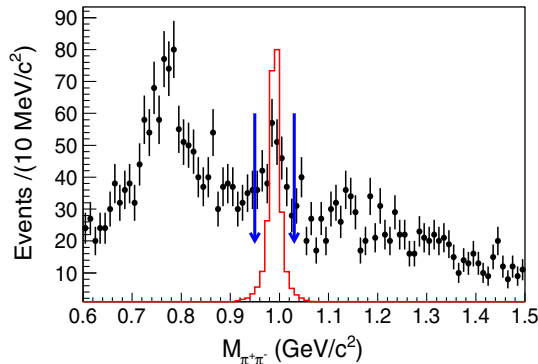


FIG. 3. The $\pi^+\pi^-$ invariant mass distribution for the events with $\pi^+\pi^-\pi^0$ invariant mass within the region of $[1.20, 2.00]$ GeV/c^2 . Dots with error bars are data, the solid line is the MC $f_0(980)$ signal shape, and the region between the arrows is the $f_0(980)$ mass window.

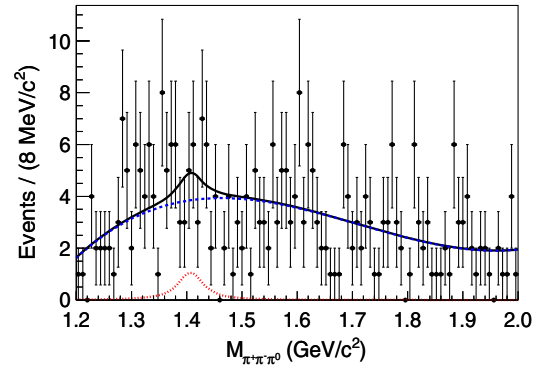


FIG. 4. Fit to the $\pi^+\pi^-\pi^0$ mass distribution in the $\eta(1405)$ region for events satisfying $|M_{\pi^+\pi^-} - m_{f_0}| < 0.04 \text{ GeV}/c^2$. The dots with error bars are data, the solid curve shows the result of unbinned maximum likelihood fit, the dotted curve is the $\eta(1405)$ signal shape, and the short-dashed curve is the background.

observed in $J/\psi \rightarrow \gamma\eta(1405)$, $\eta(1405) \rightarrow f_0(980)\pi^0$ [12]. After requiring the $\pi^+\pi^-$ invariant mass to satisfy $|M_{\pi^+\pi^-} - m_{f_0}| < 0.04 \text{ GeV}/c^2$, where m_{f_0} is the nominal mass of $f_0(980)$ [2], there is no apparent $\eta(1405)$ signal in the $M_{\pi^+\pi^-\pi^0}$ distribution, shown in Fig. 4. The background events are investigated using π^0 sidebands ($0.100 < M_{\gamma\gamma} < 0.115 \text{ GeV}/c^2$ and $0.155 < M_{\gamma\gamma} < 0.170 \text{ GeV}/c^2$), $f_0(980)$ sidebands ($0.90 < M_{\pi^+\pi^-} < 0.94 \text{ GeV}/c^2$ and $1.04 < M_{\pi^+\pi^-} < 1.08 \text{ GeV}/c^2$), and the inclusive MC decays, and no obvious peaking structures are observed around $1.4 \text{ GeV}/c^2$.

Using the same approach as in the search for $\eta_c \rightarrow \pi^+\pi^-\pi^0$, we set an upper limit at the 90% C.L. on the branching fraction for the decay $\psi(3686) \rightarrow \gamma\eta(1405)$, $\eta(1405) \rightarrow f_0(980)\pi^0$ by fitting the distribution of $\pi^+\pi^-\pi^0$ invariant mass. The fit curve is shown in Fig. 4, where the signal shape of the $\eta(1405)$ is obtained from MC simulation in which the mass and width are fixed to the world average values [2], and the background is modeled by a third order Chebychev polynomial function. Fit-related uncertainties are determined by performing various fits with variations of the $\eta(1405)$ mass and width, different fit ranges and alternative background functions. The largest upper limit on the yield of $\eta(1405)$ at the 90% C.L. is $N_{\eta(1405)}^{UL} = 38$.

IV. SYSTEMATIC UNCERTAINTIES

The systematic uncertainties in branching fraction measurements mainly come from the tracking, photon detection, and particle identification (PID) efficiencies, the 4C kinematic fit, the π^0 mass window requirement, the uncertainties of $\mathcal{B}(\pi^0 \rightarrow \gamma\gamma)$ and the number of $\psi(3686)$ events, and the fitting related uncertainties.

The MDC tracking efficiency is studied with clean channels of $J/\psi \rightarrow p\bar{p}\pi^+\pi^-$ and $J/\psi \rightarrow \rho\pi$ [9], and the

MC simulation is found to agree with data within 1%. Therefore 2% is taken as the systematic uncertainty for the two charged tracks in the final states.

The photon detection efficiency is studied with the control sample $J/\psi \rightarrow \pi^+\pi^-\pi^0$ [30]. The difference between data and MC is less than 1% per photon. Therefore 3% is assigned as the systematic uncertainty from the three photons.

The π^\pm particle identification efficiency is studied using a clean control sample of $J/\psi \rightarrow \rho\pi$ events, and the PID efficiency for data agrees with that of the Monte Carlo simulation within 1%. In this analysis, two charged tracks are identified as pions, so 2% is taken as the systematic uncertainty.

The uncertainty associated with the 4C kinematic fit comes from the inconsistency between data and MC simulation; this difference is reduced by correcting the track helix parameters of the MC simulation, as described in detail in Ref. [31]. The correction parameters for pions are obtained by using control samples of $\psi(3686) \rightarrow \pi^+\pi^-\pi^0$. In this analysis, the efficiency obtained from the corrected MC samples is taken as the nominal value, and we take the differences between the efficiencies with and without correction, 4.5% for $\eta_c \rightarrow \pi^+\pi^-\pi^0$, and 3.1% for $\eta(1405) \rightarrow f_0(980)\pi^0$, as the systematic uncertainties.

The uncertainty due to the width of $f_0(980)$ is estimated by varying its parameters by 1σ in the MC simulation, where the parameters are obtained from the fit to data. The relative change of the detection efficiency, 5.4%, is taken as the corresponding systematic uncertainty.

The uncertainty related with the π^0 mass window requirement is studied with control samples of $\psi(3686) \rightarrow \pi^+\pi^-\pi^0$ for both data and MC simulation. We fit the $\gamma\gamma$ invariant mass distribution to determine the π^0 signal yields, and the π^0 efficiency is the ratio of the π^0 yields with and without the π^0 mass window requirement, where the π^0 yield is obtained by integrating the fitted signal shape. The difference in efficiencies between data and MC simulation, 0.8%, is assigned as the systematic uncertainty.

The branching fraction uncertainty of $\pi^0 \rightarrow \gamma\gamma$ is taken from the PDG [2] and is 0.03%. The uncertainty of the number of $\psi(3686)$ events is 0.65% [16].

For $\eta_c \rightarrow \pi^+\pi^-\pi^0$ and $\eta(1405) \rightarrow f_0(980)\pi^0$, the uncertainties from the fitting range, background shape, and the signal shape have already been considered, since we select the maximum upper limit from amongst various fits described above.

Table I summarizes all contributions to the systematic uncertainties on the branching fraction measurements. In each case, the total systematic uncertainty is given by the quadratic sum of the individual contributions, assuming all sources to be independent.

TABLE I. Summary of systematic uncertainty sources and their contributions (in %).

Source	$\eta_c \rightarrow \pi^+\pi^-\pi^0$	$\eta(1405) \rightarrow f_0(980)\pi^0$
MDC tracking	2.0	2.0
Photon detection	3.0	3.0
Particle ID	2.0	2.0
4C kinematic fit	4.5	3.1
π^0 mass window	0.8	0.8
Width of $f_0(980)$...	5.4
$B(\pi^0 \rightarrow \gamma\gamma)$	0.03	0.03
Number of $\psi(3686)$	0.65	0.65
Total	6.2	7.5

V. RESULTS

To be conservative, the upper limit on the branching fraction is determined by

$$\mathcal{B}(\psi(3686) \rightarrow \gamma X) < \frac{N^{UL}}{N_{\psi(3686)} \times \varepsilon \times \mathcal{B}(\pi^0 \rightarrow \gamma\gamma) \times (1 - \delta_{\text{sys}})}, \quad (2)$$

where X stands for $\eta_c(\eta_c \rightarrow \pi^+\pi^-\pi^0)$ or $\eta(1405)(\eta(1405) \rightarrow f_0(980)\pi^0 \rightarrow \pi^+\pi^-\pi^0)$, ε is the detection efficiency obtained from the MC simulation and δ_{sys} is the total systematic uncertainty.

The detection efficiencies are 18.4% and 18.5% for $\eta_c \rightarrow \pi^+\pi^-\pi^0$ and $\eta(1405) \rightarrow f_0(980)\pi^0$, respectively, which are determined with MC simulation by assuming the polar angle of radiative photon follows the distribution $1 + \cos^2\theta_\gamma$. The upper limits at the 90% C.L. on $\mathcal{B}(\psi(3686) \rightarrow \gamma\eta_c) \times \mathcal{B}(\eta_c \rightarrow \pi^+\pi^-\pi^0)$ and $\mathcal{B}(\psi(3686) \rightarrow \gamma\eta(1405)) \times \mathcal{B}(\eta(1405) \rightarrow f_0(980)\pi^0) \times \mathcal{B}(f_0(980) \rightarrow \pi^+\pi^-)$ are calculated to be 1.6×10^{-6} and 5.0×10^{-7} , respectively.

VI. SUMMARY

Using 448.1×10^6 $\psi(3686)$ events accumulated with the BESIII detector, the search for $\eta_c \rightarrow \pi^+\pi^-\pi^0$ is performed for the first time. No obvious η_c signal is seen in the $\pi^+\pi^-\pi^0$ mass spectrum, and the 90% C.L. upper limit on $\mathcal{B}(\psi(3686) \rightarrow \gamma\eta_c) \times \mathcal{B}(\eta_c \rightarrow \pi^+\pi^-\pi^0)$ is 1.6×10^{-6} . Using the branching fraction of $\psi(3686) \rightarrow \gamma\eta_c$, $[3.4 \pm 0.5] \times 10^{-3}$, the upper limit for $\mathcal{B}(\eta_c \rightarrow \pi^+\pi^-\pi^0)$ is calculated to be 5.5×10^{-4} . We also search for $\psi(3686) \rightarrow \gamma\eta(1405)$, $\eta(1405) \rightarrow f_0(980)\pi^0$. No obvious structure around the $\eta(1405)$ is observed, and the 90% C.L. upper limit on $\mathcal{B}(\psi(3686) \rightarrow \gamma\eta(1405)) \times \mathcal{B}(\eta(1405) \rightarrow f_0(980)\pi^0) \times \mathcal{B}(f_0(980) \rightarrow \pi^+\pi^-)$ is 5.0×10^{-7} . In addition, based on the measurement in J/ψ decays [12], the ratio of $\frac{\mathcal{B}(\psi(3686) \rightarrow \gamma\eta(1405))}{\mathcal{B}(J/\psi \rightarrow \gamma\eta(1405))}$ is calculated to be less than 3.3×10^{-2} ,

which indicates that this process also violates the “12% rule”.

ACKNOWLEDGMENTS

The BESIII collaboration thanks the staff of BEPCII and the IHEP computing center for their strong support. This work is supported in part by National Key Basic Research Program of China under Contract No. 2015CB856700; National Natural Science Foundation of China (NSFC) under Contracts No. 11735014, No. 11675184, No. 11235011, No. 11322544, No. 11335008, No. 11425524, No. 11635010; the Chinese Academy of Sciences (CAS) Large-Scale Scientific Facility Program; the CAS Center for Excellence in Particle Physics (CCEPP); the Collaborative Innovation Center for Particles and Interactions (CICPI); Joint Large-Scale Scientific Facility Funds of the NSFC and CAS under Contracts No. U1232201, No. U1332201, No. U1532257, No. U1532258; CAS under Contracts No. KJCX2-YW-N29,

No. KJCX2-YW-N45, No. QYZDJ-SSW-SLH003; 100 Talents Program of CAS; National 1000 Talents Program of China; INPAC and Shanghai Key Laboratory for Particle Physics and Cosmology; German Research Foundation DFG under Contracts No. Collaborative Research Center CRC 1044, No. FOR 2359; Istituto Nazionale di Fisica Nucleare, Italy; Koninklijke Nederlandse Akademie van Wetenschappen (KNAW) under Contract No. 530-4CDP03; Ministry of Development of Turkey under Contract No. DPT2006K-120470; National Science and Technology fund; The Swedish Research Council; U.S. Department of Energy under Contracts No. DE-FG02-05ER41374, No. DE-SC-0010118, No. DE-SC-0010504, No. DE-SC-0012069; University of Groningen (RuG) and the Helmholtzzentrum fuer Schwerionenforschung GmbH (GSI), Darmstadt; WCU Program of National Research Foundation of Korea under Contract No. R32-2008-000-10155-0.

-
- [1] R. Partridge *et al.*, *Phys. Rev. Lett.* **45**, 1150 (1980).
 [2] C. Patrignani *et al.* (Particle Data Group), *Chin. Phys. C* **40**, 100001 (2016) and 2017 update.
 [3] A. Rusetsky (Bonn University), *Proc. Sci.*, CD09 (2009) 071.
 [4] D. J. Gross, S. B. Treiman, and F. Wilczek, *Phys. Rev. D* **19**, 2188 (1979).
 [5] P. Kroll, *Int. J. Mod. Phys. A* **20**, 331 (2005).
 [6] M. Ablikim *et al.* (BESIII Collaboration), *Phys. Rev. D* **87**, 092011 (2013).
 [7] M. Ablikim *et al.* (BESIII Collaboration), *Phys. Rev. D* **87**, 032006 (2013).
 [8] M. Ablikim *et al.* (BESIII Collaboration), *Phys. Rev. D* **87**, 012009 (2013).
 [9] M. Ablikim *et al.* (BESIII Collaboration), *Phys. Rev. Lett.* **112**, 251801 (2014).
 [10] M. Ablikim *et al.* (BESIII Collaboration), *Phys. Rev. D* **92**, 012014 (2015).
 [11] M. Ablikim *et al.* (BESIII Collaboration), *Phys. Rev. Lett.* **118**, 012001 (2017).
 [12] M. Ablikim *et al.* (BESIII Collaboration), *Phys. Rev. Lett.* **108**, 182001 (2012).
 [13] J.-J. Wu, X.-H. Liu, Q. Zhao, and B.-S. Zou, *Phys. Rev. Lett.* **108**, 081803 (2012).
 [14] X.-G. Wu, J.-J. Wu, Q. Zhao, and B.-S. Zou, *Phys. Rev. D* **87**, 014023 (2013).
 [15] X.-H. Liu, M. Oka, and Q. Zhao, *Phys. Lett. B* **753**, 297 (2016).
 [16] M. Ablikim *et al.* (BESIII Collaboration), arXiv:1709.03653.
 [17] M. Ablikim *et al.* (BESIII Collaboration), *Nucl. Instrum. Methods Phys. Res., Sect. A* **614**, 345 (2010).
 [18] C. Zhang, *Sci. China Phys. Mech. Astron.* **53**, 2084 (2010).
 [19] T. Appelquist and H. D. Politzer, *Phys. Rev. Lett.* **34**, 43 (1975).
 [20] A. De Rujula and S. L. Glashow, *Phys. Rev. Lett.* **34**, 46 (1975).
 [21] M. Ablikim *et al.* (BESIII Collaboration), *Phys. Rev. D* **95**, 052003 (2017).
 [22] S. Agostinelli *et al.* (GEANT4 Collaboration), *Nucl. Instrum. Methods Phys. Res., Sect. A* **506**, 250 (2003).
 [23] S. Jadach, B. F. L. Ward, and Z. Wař, *Comput. Phys. Commun.* **130**, 260 (2000).
 [24] S. Jadach, B. F. L. Ward, and Z. Wař, *Phys. Rev. D* **63**, 113009 (2001).
 [25] P. Rong-Gang, *Chin. Phys. C* **32**, 599 (2008).
 [26] D. J. Lange, *Nucl. Instrum. Methods Phys. Res., Sect. A* **462**, 152 (2001).
 [27] J.-C. Chen, G.-S. Huang, X.-R. Qi, D.-H. Zhang, and Y.-S. Zhu, *Phys. Rev. D* **62**, 034003 (2000).
 [28] V. V. Anashin *et al.* (KEDR Collaboration), *Int. J. Mod. Phys. Conf. Ser.* **02**, 188 (2011).
 [29] M. Ablikim *et al.* (BESIII Collaboration), *Chin. Phys. C* **37**, 063001 (2013).
 [30] M. Ablikim *et al.* (BESIII Collaboration), *Phys. Rev. D* **92**, 052003 (2015).
 [31] M. Ablikim *et al.* (BESIII Collaboration), *Phys. Rev. D* **87**, 012002 (2013).